Dispersion relation and instability for an anisotropic non-uniform flowing plasma

Min Uk Lee[1], **Gunsu S. Yun**[2,3], **and Jeong-Young Ji**[1]

[1] Department of Physics, Utah State University, Logan, Utah 84322, USA

[2] Department of Physics, Pohang University of Science and Technology, Pohang, Gyeongbuk 37673, Republic of Korea

[3] Division of Advanced Nuclear Engineering, Pohang University of Science and Technology, Pohang, Gyeongbuk 37673, Republic of Korea

E-mail: `min.uk.lee@usu.edu, gunsu@postech.ac.kr, j.ji@usu.edu`

August 2022

Abstract. A generalized formula for wave instability is developed for an anisotropic non-uniform plasma with finite flows and temperatures. Six-moment fluid equations are solved to give the analytic expression for wave instability in arbitrarily non-uniform plasmas. The analytic formula explicitly states the dependence of wave instability on non-uniformities of number density, flow velocity, and anisotropic or isotropic pressure. The accuracy of formalism is verified by a numerical calculation of implicit dispersion relations in complex Fourier space. The analysis shows that non-uniformity plays a critical role in plasma instability, while the flow velocity and anisotropic pressures determine the growth rate of the instability. The instability diagram and associated instability criterion for anisotropy-driven instability are introduced as applications of the formalism.

Keywords: plasma instability, instability criteria, fluid wave, plasma flow, anisotropic pressure

Submitted to: *Plasma Phys. Control. Fusion*

1. Introduction

Plasma waves have been investigated to understand the dynamical behavior of plasma. Fourier analysis of Boltzmann equation or fluid equations shows that most fundamental plasma waves, such as Bernstein and cold waves, are stable in a uniform plasma. [1] However, the waves in a non-uniform plasma can be unstable, [2–5] and the stability can be modified by a finite flow or an anisotropic pressure. [6–8] An anisotropy effect should be taken into account for a strongly magnetized plasma. [9–11]

Plasma instability has been studied for several decades in order to control and understand plasmas. [12–14] If a perturbation in a plasma exponentially grows due to instability, the perturbation can trigger the disruption of the plasma. In order to achieve a stable plasma in a nuclear fusion device, the stability criterion should be understood. Since electromagnetic fields can be enhanced by an instability, the instability analysis can be used to interpret the signals from plasmas. Diagnostics for fusion devices have been developed to examine plasma instability via electromagnetic waves. [15–17] The waves from space have been measured to investigate the space or astrophysical plasmas. [18–21]

By analyzing the Vlasov equation, the effects of non-uniform flow and temperature on wave properties have been studied for a specific plasma flow, wave mode, and frequency regime. [22–25] On the other hand, a generalized dielectric tensor and a dispersion relation have been derived for plasmas with non-uniform densities, time-varying flows, and anisotropic temperatures. [8, 26] In the kinetic analysis, an adequate distribution function should be adopted to satisfy the Vlasov equation. For example, a ring-beam distribution [27, 28] was adopted for fusion-born ions in large tokamak plasmas [29], and a shifted Maxwellian distribution with the guiding center coordinate was adopted for a sheared flow [24]. The Maxwellian distribution function can be a valid solution for a specific situation where plasma is uniform. However, a non-Maxwellian distribution function should be considered for a general situation where plasma is non-uniform with an arbitrary flow and anisotropic temperature. As a result, a dispersion relation becomes more complicated and impractical to implement for arbitrarily non-uniform plasmas.

One simpler way of analyzing the wave is to solve fluid equations with appropriate closures, such as adiabatic equations of state [30,31]. In order to develop a comprehensive and practical formalism for wave dispersion relation and instability, we solve the fluid equations for collisionless plasmas with a non-uniform flow and an anisotropic non-uniform pressure. Instead of using the adiabatic equations of state restricted to an $\mathbf{E} \times \mathbf{B}$ flow [30, 32] and Poisson's equation for electrostatic approximation, we fully solve the continuity, momentum, pressure, and Maxwell's equations for arbitrary density, flow, pressure, and electromagnetic fields with a six-moment fluid approach.

The formalism presented in this work can be applied to general fluid plasmas with arbitrary non-uniformity. Classical instabilities in fluid plasmas were studied separately with ad hoc closures and restrictions such as ideal MHD approximation, $\mathbf{E} \times \mathbf{B}$ flow only, isotropic condition, and electrostatic approximation [33]. However, these restrictions are too strong for practical applications. The exact $\mathbf{E} \times \mathbf{B}$ drift of each species without any other flow motions is valid for the idealized MHD approximation, not for the real plasmas. Many plasmas in nature and experiments flow non-uniformly, and there are different types of flows, such as diamagnetic drift, polarization drift, and parallel flows along a magnetic field line. Pressure can be anisotropic in a magnetized plasma. Furthermore, the electrostatic approximation cannot describe actual electromagnetic phenomena in plasmas. The explicit formula in this work can accurately describe the instability of general fluid waves in non-uniform plasmas without any spatial constraints on density, flow, pressure, and electromagnetic fields.

In section 2, a generalized dielectric tensor and a dispersion relation are obtained from the fluid equations. Since the dispersion relation is written in implicit form, the Fourier mode must be found numerically by scanning the complex Fourier space. In section 3, we derive the explicit functions of non-uniform fluid variables for the complex Fourier modes. The result obtained using the formula is in good agreement with the numerical results obtained from the implicit dispersion relation. It is shown that the formula is valid even for the extremely non-uniform supersonic plasma. The explicit forms make it feasible to directly evaluate the effects of fluid quantities on plasma instability. Section 4 summarizes the formalism and discusses future work to improve the instability analysis of fluid waves in more general situations.

2. Dispersion relation and Fluid equations

A plasma dispersion relation is derived from fluid equations, Faraday's law, and Ampère's law as

$$\mathcal{D}(\omega,\mathbf{k}) = \det\left(\mathbf{nn} - n^2\mathsf{I} + \mathsf{K}\right) = 0, \tag{1}$$

where ω is the wave frequency, $\mathbf{k}$ is the wavenumber, $\mathbf{n} = c\mathbf{k}/\omega$ is the refractive index, c is the speed of light, $\mathsf{K} = \mathsf{I} - \sigma/\mathrm{i}\varepsilon_0\omega$ is the dielectric tensor, I is the identity tensor, σ is the conductivity, and ε_0 is the vacuum permittivity. The conductivity is defined by $\mathbf{J}_1 = \sum_a q_a\left(n_{a0}\mathbf{u}_{a1} + n_{a1}\mathbf{u}_{a0}\right) = \sigma\cdot\mathbf{E}_1$, where $\mathbf{J}$ is the current density, q_a is the charge, $n_a = \int f_a\mathrm{d}\mathbf{v}$ is the number density ($f_a = f_a(t,\mathbf{x},\mathbf{v})$ is the distribution function), $\mathbf{u}_a = \int \mathbf{v}f_a\mathrm{d}\mathbf{v}/n_a$ is the flow velocity, $\mathbf{E}$ is the electric field, and the subscript a denotes a species. The subscript 0 denotes an equilibrium quantity and the subscript 1 denotes a Fourier mode $\exp(\mathrm{i}\mathbf{k}\cdot\mathbf{x} - \mathrm{i}\omega t)$. For the Fourier analysis, we consider a situation where $|\mathbf{k}\cdot\nabla\varphi|/k|\nabla\varphi| \ll 1$ for any fluid quantity φ, so that the wave propagation parallel to the non-uniform direction is ignored. The dielectric tensor K in equation (1) can be obtained from fluid equations.

We solve the six-moment fluid equations for n_a, $\mathbf{u}_a$, and the anisotropic pressures $p_a^{\perp} = m_a\int w_{a\perp}^2 f_a\mathrm{d}\mathbf{v}/2$ and $p_a^{\parallel} = m_a\int w_{a\parallel}^2 f_a\mathrm{d}\mathbf{v}$, where m_a is the mass, $\mathbf{w}_a = \mathbf{v} - \mathbf{u}_a$ is the random velocity, $\mathbf{w}_{a\perp} = \mathbf{w}_a - \mathbf{w}_{a\parallel}$, $\mathbf{w}_{a\parallel} = \mathbf{w}_a\cdot\hat{z}\hat{z}$, and $\hat{z} = \mathbf{B}_0/B_0$ is the unit vector in the direction of the magnetic field $\mathbf{B}_0$. The equilibrium continuity equation $\nabla\cdot(n_{a0}\mathbf{u}_{a0}) = 0$ gives the relation

$$\kappa_{na}\cdot\mathbf{u}_{a0} = \nabla\cdot\mathbf{u}_{a0}, \tag{2}$$

where $\kappa_{na} = -(\nabla n_{a0})/n_{a0}$. Using equation 2, the linearized continuity equation can be written in the form

$$\frac{n_{a1}}{n_{a0}} = \frac{\mathbf{k} + \mathrm{i}\kappa_{na}}{\omega_{Da} + \mathrm{i}\kappa_{na}\cdot\mathbf{u}_{a0}}\cdot\mathbf{u}_{a1}, \tag{3}$$

where $\omega_{Da} = \omega - \mathbf{k}\cdot\mathbf{u}_{a0}$ is the Doppler-shifted frequency. When the perturbed flow velocity $\mathbf{u}_{a1}$ is expressed by a mobility tensor μ_a as

$$\mathbf{u}_{a1} = \mu_a\cdot\mathbf{E}_1, \tag{4}$$

the combination of equations (3) and (4) with $\mathsf{K} = \mathsf{I} - \sigma/\mathrm{i}\varepsilon_0\omega$ and $\sigma\cdot\mathbf{E}_1 = \sum_a q_a(n_{a0}\mathbf{u}_{a1} + n_{a1}\mathbf{u}_{a0})$ gives the general form for the dielectric tensor

$$\mathsf{K} = \mathsf{I} - \frac{1}{\mathrm{i}\varepsilon_0\omega}\sum_a q_a n_{a0}\left(\mathsf{I} + \frac{\mathbf{u}_{a0}\left(\mathbf{k} + \mathrm{i}\kappa_{na}\right)}{\omega_{Da} + \mathrm{i}\kappa_{na}\cdot\mathbf{u}_{a0}}\right)\cdot\mu_a. \tag{5}$$

The mobility tensor in equation (5) is determined by the momentum equation. The equilibrium momentum equation is

$$\frac{\nabla\cdot\mathsf{p}_{a0}}{m_a n_{a0}} = -\mathbf{u}_{a0}\cdot\nabla\mathbf{u}_{a0} + \frac{q_a}{m_a}\left(\mathbf{E}_0 + \mathbf{u}_{a0}\times\mathbf{B}_0\right), \tag{6}$$

where $\mathsf{p}_a = p_a^{\perp}\left(\mathsf{I}-\hat{z}\hat{z}\right) + p_a^{\parallel}\hat{z}\hat{z}$ is the pressure tensor. In this work, we ignore the off-diagonal elements of the pressure tensor and the geometric effects associated with the unit vector $\mathbf{B}_0/B_0$ (for example, $\nabla(\mathbf{B}_0/B_0) = 0$). The off-diagonal elements can be ignored when a plasma is not too far from bi-Maxwellian or Maxwellian. The anisotropic diagonal pressure can be established by the background magnetic or electric field [11, 30, 34], anisotropic heating [35, 36], and expansion or compression of a plasma [37, 38]. When the distribution function is far from the bi-Maxwellian so that the off-diagonal elements are non-negligible compared to the diagonal elements, one has to take into account the viscosity tensor $\pi_a = m_a\int\left(\mathbf{w}_a\mathbf{w}_a - w_a^2\mathsf{I}/3\right)f_a\mathrm{d}\mathbf{v}$.

Using equations (3), (6), and the Faraday's law $\mathbf{B}_1 = \mathbf{k}\times\mathbf{E}_1/\omega$, the linearized equation of motion is written as

$$\begin{aligned}&\left\{\mathsf{I} + \mathrm{i}\frac{\omega_{ca}}{\omega_{Da}}\hat{z}\times\mathsf{I}\right.\\ &\left.\quad + \mathrm{i}\frac{1}{\omega_{Da}}\left[\left(\nabla\mathbf{u}_{a0}\right)^{\mathrm{T}} - \frac{\nabla\cdot\mathsf{p}_{a0}}{m_a n_{a0}}\frac{\mathbf{k}+\mathrm{i}\kappa_{na}}{\omega_{Da}+\mathrm{i}\kappa_{na}\cdot\mathbf{u}_{a0}}\right]\right\}\cdot\mathbf{u}_{a1}\\ &\quad = \mathrm{i}\frac{q_a}{m_a\omega}\left(\mathsf{I} + \frac{\mathbf{k}\mathbf{u}_{a0}}{\omega_{Da}}\right)\cdot\mathbf{E}_1 + \frac{1}{\omega_{Da}}\frac{\mathbf{k}_{\perp}p_{a1}^{\perp} + \mathbf{k}_{\parallel}p_{a1}^{\parallel}}{m_a n_{a0}},\end{aligned} \tag{7}$$

where $\omega_{ca} = q_a B_0/m_a$ is the cyclotron frequency and the superscript T means a transpose. Please note that the detailed derivations of equations (7), (10)-(14) in this paragraph are provided in the appendix. In the Cartesian coordinate, $\hat{z}\times\mathsf{I} = \hat{y}\hat{x} - \hat{x}\hat{y}$ and $[(\nabla\mathbf{u}_{a0})^{\mathrm{T}}]_{\alpha\beta} = \partial_\beta u_{a0\alpha}$, where $\partial_\beta = \partial/\partial\beta$ and $\alpha,\beta = x,y,z$. Equation (7) gives the mobility when the anisotropic pressure elements $p_{a1}^{\perp}$ and $p_{a1}^{\parallel}$ are closed. The anisotropic pressure is determined by the pressure equations,

$$\frac{\mathrm{d}p_a^{\perp}}{\mathrm{d}t} + 2p_a^{\perp}\nabla\cdot\mathbf{u}_a - p_a^{\perp}\partial_{\parallel}u_{a\parallel} + \nabla\cdot\mathbf{q}_a^{\perp} = 0, \tag{8}$$

$$\frac{\mathrm{d}p_a^{\parallel}}{\mathrm{d}t} + p_a^{\parallel}\nabla\cdot\mathbf{u}_a + 2p_a^{\parallel}\partial_{\parallel}u_{a\parallel} + \nabla\cdot\mathbf{q}_a^{\parallel} = 0, \tag{9}$$

where $\mathrm{d}/\mathrm{d}t = \partial/\partial t + \mathbf{u}_a\cdot\nabla$, $\partial_{\parallel}u_{\parallel} = \hat{z}\cdot\nabla\mathbf{u}\cdot\hat{z}$, and $\mathbf{q}_a^{\perp} = m_a\int w_{a\perp}^2\mathbf{w}_a f_a\mathrm{d}\mathbf{v}/2$ and $\mathbf{q}_a^{\parallel} = m_a\int w_{a\parallel}^2\mathbf{w}_a f_a\mathrm{d}\mathbf{v}$ are the heat fluxes. Note that equations (8) and (9) reduce to the double adiabatic equations [30] for only $\mathbf{E}\times\mathbf{B}$ drift with or without a uniform parallel flow ($\mathbf{E}+\mathbf{u}_a\times\mathbf{B} = 0$). This limitation is too severe for real plasmas of interest. For a general flow $\mathbf{u}_a$, equations (8) and (9) should be fully solved for $p_a^{\perp}$ and $p_a^{\parallel}$. In this work, we consider a general flow and linearize equations (8) and (9) to write

$$\frac{p_{a1}^{\perp}}{p_{a0}^{\perp}} = \frac{2\mathbf{k}-\mathbf{k}_{\parallel}+\mathrm{i}\kappa_{p^{\perp}a}}{\omega_{Da}+\mathrm{i}\,2\nabla\cdot\mathbf{u}_{a0}-\mathrm{i}\,\partial_{\parallel}u_{a0\parallel}}\cdot\mathbf{u}_{a1}, \tag{10}$$

$$\frac{p_{a1}^{\parallel}}{p_{a0}^{\parallel}} = \frac{\mathbf{k}+2\mathbf{k}_{\parallel}+\mathrm{i}\kappa_{p^{\parallel}a}}{\omega_{Da}+\mathrm{i}\nabla\cdot\mathbf{u}_{a0}+\mathrm{i}\,2\partial_{\parallel}u_{a0\parallel}}\cdot\mathbf{u}_{a1}, \tag{11}$$

where $\kappa_{p^{\perp}a} = -(\nabla p_{a0}^{\perp})/p_{a0}^{\perp}$, $\kappa_{p^{\parallel}a} = -(\nabla p_{a0}^{\parallel})/p_{a0}^{\parallel}$, and we use the 6-moment (n_a, $\mathbf{u}_a$, $p_a^{\perp}$, $p_a^{\parallel}$) approximation . This approximation can be valid when the phase speed ω/k is much faster than the thermal speeds $v_{T^{\perp}a} = (2T_{a0}^{\perp}/m_a)^{1/2}$ and $v_{T^{\parallel}a} = (2T_{a0}^{\parallel}/m_a)^{1/2}$, [23, 39] where $T_a^{\perp} = p_a^{\perp}/n_a$ and $T_a^{\parallel} = p_a^{\parallel}/n_a$ are the anisotropic temperatures ($\kappa_{p^{\perp}a} = \kappa_{na} + \kappa_{T^{\perp}a}$, $\kappa_{p^{\parallel}a} = \kappa_{na} + \kappa_{T^{\parallel}a}$). With equations (10) and (11), equation (7) can be rearranged to give the mobility

$$\mu_a = \mathrm{i}\frac{q_a}{m_a\omega}\left(\mathsf{I}+\mathrm{i}\frac{\omega_{ca}}{\omega_{Da}}\hat{z}\times\mathsf{I}+\mathrm{i}\frac{\Gamma_a}{\omega_{Da}}\right)^{-1}\cdot\left(\mathsf{I}+\frac{\mathbf{k}\,\mathbf{u}_{a0}}{\omega_{Da}}\right). \tag{12}$$

The effects of non-uniform density, flow, and anisotropic pressure are involved in the coefficient Γ_a as

$$\begin{aligned}\Gamma_a = (\nabla\mathbf{u}_{a0})^{\mathrm{T}} &- \frac{\nabla\cdot\mathsf{p}_{a0}}{m_a n_{a0}}\frac{\mathbf{k}+\mathrm{i}\kappa_{na}}{\omega_{Da}+\mathrm{i}\kappa_{na}\cdot\mathbf{u}_{a0}}\\ &+\frac{\mathrm{i}\mathbf{k}_{\perp}\left(2\mathbf{k}-\mathbf{k}_{\parallel}+\mathrm{i}\kappa_{p^{\perp}a}\right)v_{T^{\perp}a}^2/2}{\omega_{Da}+\mathrm{i}\,2\nabla\cdot\mathbf{u}_{a0}-\mathrm{i}\,\partial_{\parallel}u_{a0\parallel}}\\ &+\frac{\mathrm{i}\mathbf{k}_{\parallel}\left(\mathbf{k}+2\mathbf{k}_{\parallel}+\mathrm{i}\kappa_{p^{\parallel}a}\right)v_{T^{\parallel}a}^2/2}{\omega_{Da}+\mathrm{i}\nabla\cdot\mathbf{u}_{a0}+\mathrm{i}\,2\partial_{\parallel}u_{a0\parallel}}.\end{aligned} \tag{13}$$

The coefficient for an isotropic pressure $\mathsf{p}_a = p_a\mathsf{I}$ ($p_a = m_a\int w_a^2 f_a \mathrm{d}\mathbf{v}/3$) is

$$\begin{aligned}\Gamma_a = (\nabla\mathbf{u}_{a0})^{\mathrm{T}} &- \frac{\nabla\cdot\mathsf{p}_{a0}}{m_a n_{a0}}\frac{\mathbf{k}+\mathrm{i}\kappa_{na}}{\omega_{Da}+\mathrm{i}\kappa_{na}\cdot\mathbf{u}_{a0}}\\ &+\frac{\mathrm{i}\mathbf{k}\,(5\mathbf{k}/3+\mathrm{i}\kappa_{pa})\,v_{Ta}^2/2}{\omega_{Da}+\mathrm{i}\,5\nabla\cdot\mathbf{u}_{a0}/3},\end{aligned} \tag{14}$$

where $\kappa_{pa} = -(\nabla p_{a0})/p_{a0}$. This is because $3\partial_{\parallel}u_{\parallel} = \nabla\cdot\mathbf{u}_a$ is the necessary condition for the isotropic condition (see equations (8) and (9) with $p_a^{\perp} = p_a^{\parallel} = p_a$). Substitution for μ_a (equations (12)-(14)) into equation (5) gives the dielectric tensor K and the associated dispersion relation (1) for the fluid wave. If the terms Γ_a and $\mathbf{u}_{a0}$ are ignored, equation (1) becomes the dispersion relation $\mathcal{D}(\omega_{\mathrm{r}},\mathbf{k}_{\mathrm{r}}) = 0$ for the cold wave without damping or instability ($\omega_{\mathrm{i}} = 0$, $\mathbf{k}_{\mathrm{i}} = 0$), where the subscripts r and i denote the real and imaginary parts. This indicates that the non-uniformity involved in Γ_a plays a key role in wave dynamics with finite ω_{i} and $\mathbf{k}_{\mathrm{i}}$. Since the fluid wave in a non-uniform plasma has an implicit dispersion relation such as $\mathcal{D}(\omega_{\mathrm{r}}+\mathrm{i}\omega_{\mathrm{i}},\mathbf{k}_{\mathrm{r}}+\mathrm{i}\mathbf{k}_{\mathrm{i}}) = 0$, the dispersion relation can be obtained numerically in complex Fourier space.

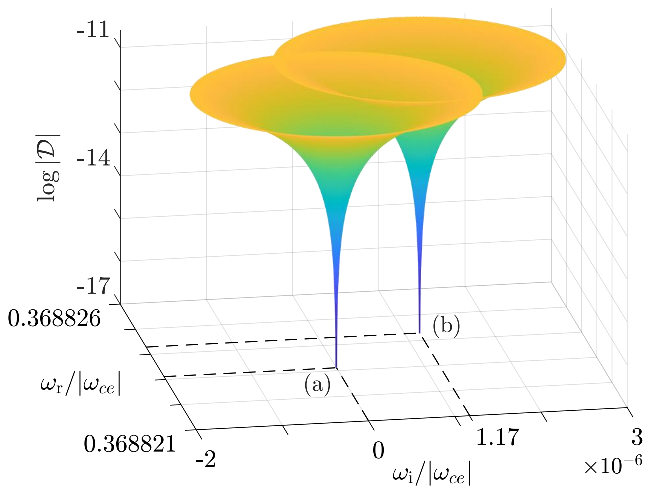

Figure 1. Comparison of whistler wave frequencies for $\mathbf{k}r_{Li} = 0.5\pi\hat{z}$ ($r_{La} = (T_{a0}^{\perp}/m_a)^{1/2}/|\omega_{ca}|$ is the Larmor radius): (a) uniform plasma, (b) non-uniform plasma with $(\nabla\mathbf{u}_{a0})/\omega_{ci} = 0.1\hat{y}(\hat{x}-\hat{y})$ for $a = e, i$. The equilibrium parameters are $n_{a0} = 10^{19}$ m^{-3}, $T_{a0}^{\parallel} = 0.8$ keV, $T_{a0}^{\perp} = 1.2$ keV, and $B_0 = 2$ T, where i denotes the deuterium ion ($q_i = -q_e$). The convergence of the numerical calculation for $\mathcal{D} \to 0$ is verified by reducing the grid sizes ($\Delta\omega_\mathrm{r}$, $\Delta\omega_\mathrm{i}$) in the frequency domain.

Figure 1 shows an example of investigating the dispersion relation $\mathcal{D}(\omega_\mathrm{r} + \mathrm{i}\omega_\mathrm{i}, \mathbf{k}_\mathrm{r}) = 0$. By scanning the complex frequency space for a given wavenumber, the whistler wave [40,41] frequencies are found for a uniform and non-uniform plasma. It is seen that the change in the real frequency due to the non-uniformity is insignificant compared to the change in the imaginary frequency. The wave frequency for the uniform plasma is pure real, whereas the frequency for the non-uniform plasma is complex with a positive imaginary part. The frequency shift from $\omega_\mathrm{i} = 0$ to $\omega_\mathrm{i} > 0$ indicates that the non-uniform plasma flow drives instability. By investigating broader frequency ranges, we can find the other waves having different complex frequencies even for the same wavenumber. The whole dispersion relation can be found by scanning a wide range of complex Fourier space. However, the broader scanning range induces a more computational load. The following section introduces an explicit formalism that can directly yield the dispersion relation.

3. Generalized formula for fluid instability

By expanding the implicit dielectric tensor in equation (5) for $\omega_\mathrm{i} \ll \omega_\mathrm{r}$, we derive an explicit dispersion relation providing an imaginary frequency for given plasma parameters. This method has the virtue that the quantitative estimate of plasma instability can be made with less computational effort. We expand the dielectric tensor K about $\Gamma_a = 0$ and $\mathbf{u}_{a0} = 0$ as $\mathsf{K} = \mathsf{K}_{(0)} + \mathsf{K}_{(1)}$, where the terms denoted by the subscripts (0) and (1) are, respectively, zeroth- and first-orders in $\Gamma_{a\alpha\beta}$ or $u_{a0\beta}$ for arbitrary α, β. The dielectric tensor $\mathsf{K}_{(0)}$ corresponds to the dielectric tensor for the cold wave, as discussed in the previous section. This approach is effectively equivalent to the expansion of K about real frequency ω_r when

$\Gamma_{a\alpha\beta}$, $\kappa_{na\alpha}u_{a0\beta}$, and the resulting $\omega_{\rm i}$ are much smaller than $\omega_{\rm r}$, since $\omega_{\rm i}$ is a linear function of $\Gamma_{a\alpha\beta}$ and $\kappa_{na\alpha}u_{a0\beta}$ (this will be shown in equations (25)-(38)). The dielectric tensor for the cold wave is, [1]

$$\mathsf{K}_{(0)} = \begin{bmatrix} S & -{\rm i}D & 0 \\ {\rm i}D & S & 0 \\ 0 & 0 & P \end{bmatrix}, \tag{15}$$

where,

$$S = 1 - \sum_a \frac{\omega_{pa}^2}{\omega^2 - \omega_{ca}^2},\ D = \sum_a \frac{\omega_{ca}}{\omega}\frac{\omega_{pa}^2}{\omega^2 - \omega_{ca}^2},\ P = 1 - \sum_a \frac{\omega_{pa}^2}{\omega^2}, \tag{16}$$

and $\omega_{pa} = (n_{a0}q_a^2/\varepsilon_0 m_a)^{1/2}$ is the plasma frequency. The remaining part $\mathsf{K}_{(1)}$ consists of the coefficients proportional to $\Gamma_{a\alpha\beta}$, $\kappa_{na\alpha}u_{a0\beta}$, and $k_\alpha u_{a0\beta}$ as

$$K_{(1)\alpha\beta} = \sum_a \frac{-\omega_{pa}^2}{\omega^2 - \omega_{ca}^2}\left(\eta_{a(1)} + \eta_{a(0)}\cdot\frac{\mathbf{k}\,\mathbf{u}_{a0}}{\omega} + \frac{\mathbf{u}_{a0}\,(\mathbf{k}+{\rm i}\kappa_{na})}{\omega}\cdot\eta_{a(0)}\right), \tag{17}$$

where

$$\eta_{a(0)} = \begin{bmatrix} 1 & {\rm i}\dfrac{\omega_{ca}}{\omega} & 0 \\ -{\rm i}\dfrac{\omega_{ca}}{\omega} & 1 & 0 \\ 0 & 0 & \dfrac{\omega^2-\omega_{ca}^2}{\omega^2} \end{bmatrix}, \tag{18}$$

$$\eta_{a(1)} = {\rm i}\begin{bmatrix} \dfrac{\Gamma_{ayy}}{\omega}+\Delta_a & \dfrac{\omega_{ca}}{\omega}\dfrac{\mathbf{k}\cdot\mathbf{u}_{a0}}{\omega} - \dfrac{\Gamma_{axy}}{\omega} + {\rm i}\dfrac{\omega_{ca}}{\omega}\Delta_a & -\dfrac{\Gamma_{axz}}{\omega} - {\rm i}\dfrac{\omega_{ca}}{\omega}\dfrac{\Gamma_{ayz}}{\omega} \\ -\dfrac{\omega_{ca}}{\omega}\dfrac{\mathbf{k}\cdot\mathbf{u}_{a0}}{\omega} - \dfrac{\Gamma_{ayx}}{\omega} - {\rm i}\dfrac{\omega_{ca}}{\omega}\Delta_a & \dfrac{\Gamma_{axx}}{\omega}+\Delta_a & -\dfrac{\Gamma_{ayz}}{\omega} + {\rm i}\dfrac{\omega_{ca}}{\omega}\dfrac{\Gamma_{axz}}{\omega} \\ -\dfrac{\Gamma_{azx}}{\omega} + {\rm i}\dfrac{\omega_{ca}}{\omega}\dfrac{\Gamma_{azy}}{\omega} & -\dfrac{\Gamma_{azy}}{\omega} - {\rm i}\dfrac{\omega_{ca}}{\omega}\dfrac{\Gamma_{azx}}{\omega} & -\dfrac{\omega^2-\omega_{ca}^2}{\omega^2}\dfrac{\Gamma_{azz}}{\omega} \end{bmatrix}, \tag{19}$$

and

$$\Delta_a = -\frac{\omega^2}{\omega^2-\omega_{ca}^2}\left[\frac{\Gamma_{axx}}{\omega} + \frac{\Gamma_{ayy}}{\omega} + {\rm i}\frac{\omega_{ca}}{\omega}\left(\frac{\Gamma_{ayx}}{\omega} - \frac{\Gamma_{axy}}{\omega}\right) + {\rm i}2\frac{\omega_{ca}^2}{\omega^2}\frac{\mathbf{k}\cdot\mathbf{u}_{a0}}{\omega}\right], \tag{20}$$

Note that this method is less accurate near the resonance $\omega^2 = \omega_{ca}^2$, since the dielectric tensor is expanded for $|\Delta_a| \ll 1$. As a consequence of the expanded dielectric tensor, the dispersion relation can be written as $\mathcal{D}(\omega,\mathbf{k}) = \mathcal{D}_{(0)} + \mathcal{D}_{(1)} = 0$. The first term $\mathcal{D}_{(0)}$ depends only on $\mathsf{K}_{(0)}$ and is written in the form

$$\mathcal{D}_{(0)}(\omega,k) = a_2 n^4 + a_1 n^2 + a_0, \tag{21}$$

where

$$\begin{aligned}
a_0 &= \left(S^2 - D^2\right) P, \\
a_1 &= \left(D^2 - S^2\right) \sin^2\theta - SP\left(1 + \cos^2\theta\right), \\
a_2 &= S\sin^2\theta + P\cos^2\theta,
\end{aligned} \tag{22}$$

and the x axis is chosen to be in the $\mathbf{k}_\perp$ direction so that $\mathbf{k} = k\sin\theta\,\hat{x} + k\cos\theta\,\hat{z}$ with $\theta = \cos^{-1}(\mathbf{k}\cdot\hat{z}/k)$. In this formalism we consider a real $\mathbf{k}$. The $\mathsf{K}_{(1)}$-dependent part of the dispersion relation is

$$\begin{aligned}
&\mathcal{D}_{(1)}(\omega,k) = \left(n^2 - S\right)\left(n_x^2 - P\right) K_{(1)xx} \\
&- \left(Sn_x^2 + Pn_z^2 - SP\right) K_{(1)yy} + \mathrm{i}D\left(n_x^2 - P\right)\left(K_{(1)xy} - K_{(1)yx}\right) \\
&+ \left[\left(n_z^2 - S\right)\left(n^2 - S\right) - D^2\right] K_{(1)zz} \\
&+ n_x n_z \left[\left(n^2 - S\right)\left(K_{(1)xz} + K_{(1)zx}\right) + \mathrm{i}D\left(K_{(1)zy} - K_{(1)yz}\right)\right].
\end{aligned} \tag{23}$$

The full dispersion relation can be decomposed as $\mathcal{D}(\omega,k) = \mathcal{D}_\mathrm{r}(\omega,k) + \mathrm{i}\mathcal{D}_\mathrm{i}(\omega,k)$, where $\mathcal{D}_\mathrm{r}$ is the part that does not contain i and $\mathcal{D}_\mathrm{i}$ is the part that contains i (for example, $\mathcal{D}_{(0)}(\omega,k) = \mathcal{D}_{(0)\mathrm{r}}(\omega,k)$ in equation (21). The real part of the Taylor expansion for $\mathcal{D}(\omega,k)$ at ω_r becomes the relations $\mathcal{D}_{(0)}(\omega_\mathrm{r},k) \simeq 0$ giving

$$k^2 \simeq \frac{\omega_\mathrm{r}^2}{c^2}\frac{-a_1 \pm \sqrt{a_1^2 - 4a_2a_0}}{2a_2}, \tag{24}$$

where the right-hand side is a function of ω_r only. The imaginary part of the expansion for $\mathcal{D}(\omega,k)$ gives the imaginary frequency

$$\omega_\mathrm{i} \simeq -\frac{\mathcal{D}_{(1)\mathrm{i}}(\omega_\mathrm{r},k)}{\partial\mathcal{D}_{(0)}/\partial\omega\big|_{\omega=\omega_\mathrm{r}}}. \tag{25}$$

The imaginary frequency ω_i can be directly evaluated by using equation (25), where ω_r and k are obtained using equation (24). For the denominator $\partial\mathcal{D}_{(0)}/\partial\omega$ associated with equation (21),

$$\frac{\partial\mathcal{D}_{(0)}}{\partial\omega} = \left(\frac{\partial a_2}{\partial\omega} - 4\frac{a_2}{\omega}\right) n^4 + \left(\frac{\partial a_1}{\partial\omega} - 2\frac{a_1}{\omega}\right) n^2 + \frac{\partial a_0}{\partial\omega}, \tag{26}$$

where the derivatives of S, D, and P with respect to ω are given as

$$\frac{\partial P}{\partial\omega} = \sum_a \frac{2\omega_{pa}^2}{\omega^3}, \tag{27}$$

$$\frac{\partial S}{\partial\omega} = \sum_a \frac{2\omega\omega_{pa}^2}{\left(\omega^2 - \omega_{ca}^2\right)^2}, \tag{28}$$

$$\frac{\partial D}{\partial\omega} = -\sum_a \frac{\omega_{ca}}{\omega}\frac{\omega_{pa}^2\left(3\omega^2 - \omega_{ca}^2\right)}{\omega\left(\omega^2 - \omega_{ca}^2\right)^2}. \tag{29}$$

For the numerator $\mathcal{D}_{(1)\mathrm{i}}$ associated with equation (23), we use the coefficients $K_{(1)\mathrm{i}xx}$, $K_{(1)\mathrm{i}yy}$, $K_{(1)\mathrm{i}zz}$, $K_{(1)\mathrm{r}xy} - K_{(1)\mathrm{r}yx}$, $K_{(1)\mathrm{i}xz} + K_{(1)\mathrm{i}zx}$, and $K_{(1)\mathrm{r}yz} - K_{(1)\mathrm{r}zy}$ as follows:

$$K_{(1)\mathrm{i}xx} = -\sum_a \frac{\omega_{pa}^2}{\omega^2 - \omega_{ca}^2}\left(\frac{\kappa_{nax}u_{a0x} + \partial_y u_{a0y}}{\omega} + F_a\right), \tag{30}$$

$$K_{(1)\mathrm{i}yy} = -\sum_a \frac{\omega_{pa}^2}{\omega^2 - \omega_{ca}^2} \left(\frac{\kappa_{nay} u_{a0y} + \partial_x u_{a0x}}{\omega} + F_a \right), \tag{31}$$

$$\begin{aligned} K_{(1)\mathrm{r}xy} - K_{(1)\mathrm{r}yx} = \sum_a \frac{\omega_{pa}^2}{\omega^2 - \omega_{ca}^2} \bigg(& \frac{\omega_{ca}}{\omega} \frac{\kappa_{na} \cdot \mathbf{u}_{a0\perp}}{\omega} \\ & + \frac{\kappa_{na} \times \kappa_{p^\perp a} \cdot \hat{z}}{2\omega^2 / v_{T^\perp a}^2} + 2 \frac{\omega_{ca}}{\omega} F_a \bigg), \end{aligned} \tag{32}$$

$$K_{(1)\mathrm{i}zz} = -\sum_a \frac{\omega_{pa}^2}{\omega^2} \frac{\left(\kappa_{na\|} - \partial_\|\right) u_{a0\|}}{\omega}, \tag{33}$$

$$\begin{aligned} K_{(1)\mathrm{i}xz} + K_{(1)\mathrm{i}zx} = & -\sum_a \frac{\omega_{pa}^2}{\omega^2 - \omega_{ca}^2} \left(G_a + \frac{\omega_{ca}}{\omega} H_a \right) \\ & -\sum_a \frac{\omega_{pa}^2}{\omega^2} \frac{\kappa_{na\|} u_{a0x}}{\omega}, \end{aligned} \tag{34}$$

$$K_{(1)\mathrm{r}yz} - K_{(1)\mathrm{r}zy} = -\sum_a \frac{\omega_{pa}^2}{\omega^2 - \omega_{ca}^2} \left(H_a + \frac{\omega_{ca}}{\omega} G_a \right), \tag{35}$$

where

$$F_a = -\frac{\omega^2}{\omega^2 - \omega_{ca}^2} \left(\frac{\nabla \cdot \mathbf{u}_{a0\perp}}{\omega} - \frac{\omega_{ca}}{\omega} \frac{\kappa_{na} \times \kappa_{p^\perp a} \cdot \hat{z}}{2\omega^2 / v_{T^\perp a}^2} \right), \tag{36}$$

$$\begin{aligned} G_a = & \frac{\left(\kappa_{nax} - \partial_x\right) u_{a0\|} - \partial_\| u_{a0x}}{\omega} \\ & - \frac{\mathbf{k} \times \kappa_{p^\perp a} \cdot \hat{y}}{2\omega^2 / v_{T^\perp a}^2} + \frac{\mathbf{k} \times \kappa_{p^\| a} \cdot \hat{y}}{2\omega^2 / v_{T^\| a}^2}, \end{aligned} \tag{37}$$

$$H_a = \frac{\kappa_{na\|} \kappa_{p^\perp ay}}{2\omega^2 / v_{T^\perp a}^2} - \frac{\kappa_{nay} \kappa_{p^\| a\|}}{2\omega^2 / v_{T^\| a}^2}, \tag{38}$$

and $\kappa_{\varphi a \alpha} = \kappa_{\varphi a} \cdot \hat{\alpha}$ for $\varphi = n, p^\perp, p^\|$ (e.g., $\kappa_{p^\| a\|} = \kappa_{p^\| a} \cdot \hat{z}$). Note that the same coefficients are derived from the isotropic condition (14), so equations (16), (21)-(38) can be used for the isotropic plasma with $\kappa_{pa} = \kappa_{p^\perp a} = \kappa_{p^\| a}$. The coefficients show that the effects of finite flow and anisotropic temperature on plasma instability are negligible if the parameters are uniform, i.e., the non-uniformity is the critical factor for the instability of fluid waves.

We can verify the instability formalism of equations (24)-(38) by comparing the analytic result from the explicit formalism to the numerical result from the implicit relation (1). In order to show the validity of the formalism, examples of the dispersion relations for the extremely non-uniform supersonic plasma are shown in figures 2-4. The species, density, temperature, and magnetic field are the same as in figure 1. The other parameters are $\mathbf{u}_{a0} = v_{T^\perp i} (\hat{x} + \hat{y}) + v_{T^\| i} \hat{z}$, $(\nabla \mathbf{u}_{a0})/\omega_{ci} = \hat{x}\hat{x} + 2\hat{y}\hat{y} - \hat{z}\hat{z} + 0.5\,(\hat{x}\hat{y} + \hat{y}\hat{x} + \hat{x}\hat{z} + \hat{y}\hat{z} - \hat{z}\hat{x} - \hat{z}\hat{y})$, $\kappa_{na} r_{Li} = \hat{x} + \hat{y} + \hat{z}$, $\kappa_{p^\perp a} r_{Li} = 2\hat{x} + 6\hat{y} + 2\hat{z}$, and $\kappa_{p^\| a} r_{Li} = \hat{x} + \hat{y} + 2\hat{z}$ for $a = e, i$. Note that the parameters are specified arbitrarily to demonstrate the accuracy of the formalism even in the extreme conditions. In a real situation, the parameters are determined by the fluid equations

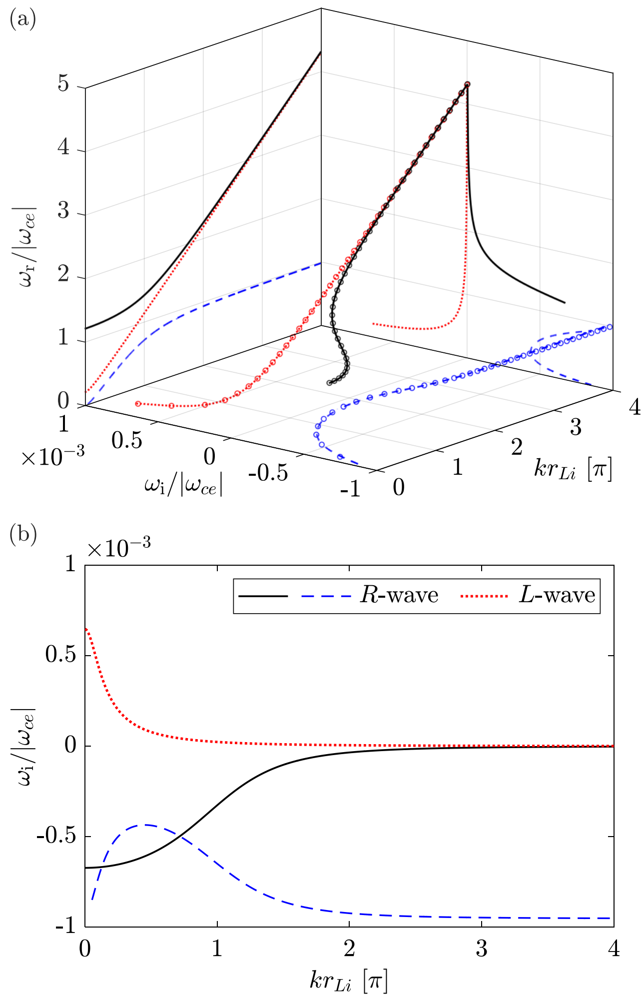

Figure 2. Non-uniform plasma dispersion relation for $\theta = 0$: (a) dispersion relation in complex Fourier space and its projection onto the k-ω_r and ω_r-ω_i spaces, (b) projection of the dispersion relation onto the k-ω_i space. The solid, dashed, and dotted lines are obtained from the dispersion formalism using equations (24)-(38), and the circle markers are obtained from the numerical scan of the Fourier space as in figure 1. The black solid lines and blue dashed lines correspond to the right-hand circularly polarized wave (R-wave, $\mathcal{D}_{(0)} = n^2 - S - D$), and the red dotted lines correspond to the left-hand circularly polarized wave (L-wave, $\mathcal{D}_{(0)} = n^2 - S + D$). The low-frequency R-wave dispersion (blue dashed line) is plotted for $\omega^2/k^2 > 10v_{T^\perp e}^2$.

in equations (2), (6), (8), and (9). Figures 2-4 demonstrate that the instability formalism is in good agreement with the implicit dispersion relation found numerically as in figure 1.

The dispersion relations in figures 3 and 4 show that the sign of the imaginary frequency depends on the wavenumber. For example, the instability criterion of the X-wave is $k > 0.5/r_{Li}$ in figure 4. The formalism also provides the instability diagram showing the relation between the non-uniformity and the wave instability. Figure 5 shows an example of an instability diagram for anisotropic non-uniform pressure. The instability diagram presents the instability criterion for a given plasma condition. As long as the derivative of the magnetic field line is ignored, the formalism provided in equations (21)-(38) corresponds

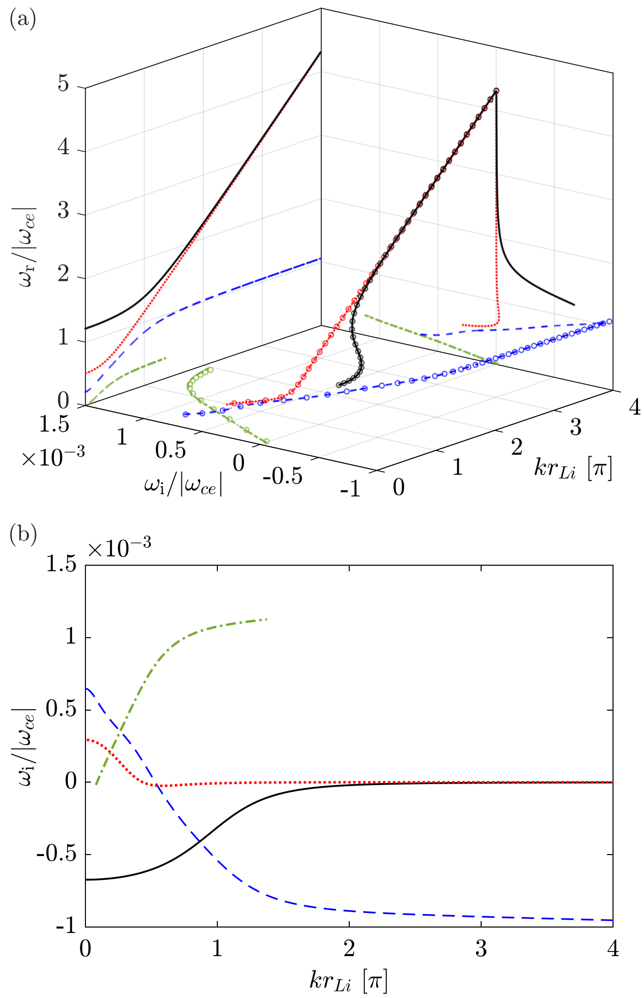

Figure 3. Non-uniform plasma dispersion relation for $\theta = \pi/4$. The plot configuration is the same as figure 2. The low-frequency wave dispersion (green dash-dotted line) is plotted for $\omega^2/k^2 > 10v_{T^\perp e}^2$.

to the generalization of the instability analysis for fluid waves. Furthermore, the closed-form expression makes it practical to analyze the instability by showing the explicit dependence of non-uniform plasma parameters on complex Fourier modes. In general, the onset criterion ($\omega_\mathrm{i} = 0$) for the fluid instability is

$$\mathcal{D}_{(1)\,\mathrm{i}}(\omega_\mathrm{r}, k) = 0, \tag{39}$$

where $\mathcal{D}_{(1)\,\mathrm{i}}(\omega_\mathrm{r}, k)$ is given by equations (23) and (30)-(38). Extended applications of the general onset criterion (39) to different fluid modes can be subject of future work.

4. Summary and conclusions

We have investigated a dispersion relation and the associated instability of plasma waves for an anisotropic non-uniform plasma with a finite flow. Plasma mobility and dielectric tensor for the non-uniform plasma are derived from Fourier-transformed fluid equations. The

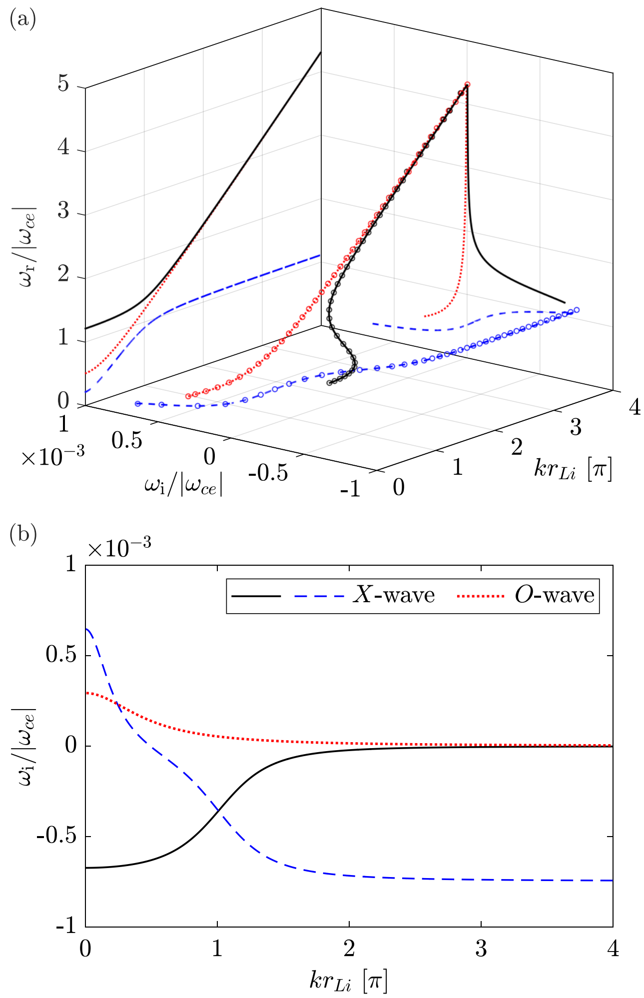

Figure 4. Non-uniform plasma dispersion relation for $\theta = \pi/2$. The plot configuration is the same as figure 2. The black solid lines and blue dashed lines correspond to the extraordinary wave (X-wave, $\mathcal{D}_{(0)} = n^2 - \left(S^2 - D^2\right)/S$), and the red dotted lines correspond to the ordinary wave (O-wave, $\mathcal{D}_{(0)} = n^2 - P$).

linearized set of continuity, momentum, and pressure equations are solved with the 6-moment approximation. The dielectric tensor is expressed in terms of the non-uniform density, flow velocity, and anisotropic pressure (equations (5), (12)-(14)). The implicit dispersion relation (1) can be solved numerically to give complex Fourier variables. The analysis shows that non-uniformity is a critical parameter for plasma instability.

We have developed an explicit formalism for plasma instability. The dependence of imaginary frequency on the non-uniformity of plasma parameters is written by expanding the dispersion relation. The plasma instability can be directly evaluated using equations (16), (22)-(38), where the coefficients demonstrate that the non-uniformity is the critical parameter of the instability. The validity of formalism has been confirmed by comparing the explicit dispersion relation (25) and the implicit dispersion relation (1). It is demonstrated that the formalism can be used to develop the instability diagram and the instability criterion for a non-uniform plasma.

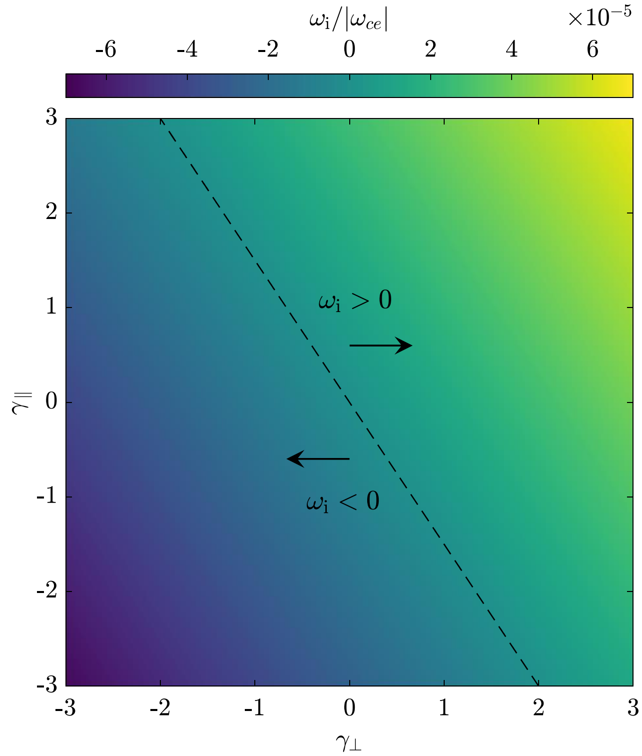

Figure 5. Instability diagram of the anisotropy-driven instability for $\theta = \pi/4$, $kr_{Li} = \pi/2$, and $\omega/|\omega_{ce}| = 0.7$. The non-uniform pressures are given as $\kappa_{p^{\perp}{}_a} r_{Li} = \gamma_{\perp}(-\hat{x}+\hat{y}+\hat{z})$ and $\kappa_{p^{\parallel}{}_a} r_{Li} = \gamma_{\parallel}(\hat{x}+\hat{y}-\hat{z})$ for $a = e, i$, and the other plasma parameters are uniform as given in figure 1(a). The dashed line is the contour of $\omega_{\rm i} = 0$, which gives the instability criterion $\gamma_{\perp} > -2\gamma_{\parallel}/3$.

The explicit expression provides an accurate and practical method for a general instability analysis of fluid waves. The method has a great advantage for assessing the instability in an arbitrarily non-uniform plasma without numerical computation. The formalism can generally be used to analyze the density-gradient instability due to non-uniform density, the temperature-gradient instability due to non-uniform temperature, and the zonal flow [42] instability due to a non-uniform flow. For example, figures 2-5 show the application of formalism to the instability analysis. The fluid instabilities driven by the comprehensive effect of density, flow, and pressure (or temperature) gradients are described as functions of non-uniform parameters and Fourier modes. The effects of the non-uniform parameters on well-known waves (R-wave, L-wave, X-wave, O-wave) and arbitrary waves are demonstrated. Figure 5 shows the instability diagram for the anisotropic-pressure-gradient instability. Using the formalism, the generalized criterion for the onset of instability is presented by equation (39). It is seen that the accurate formula for general fluid waves cannot be derived by equations of states and electrostatic approximation.

The explicit formula in this work does not include the effects of magnetic field geometry, collisions, off-diagonal elements of a pressure tensor, and non-uniformity in the direction of wave propagation. We will relax the restrictions in future work to develop a more practical and comprehensive formula. For example, equations (7)-(9) are obtained in slab geometry, where any spatial derivative of the unit vector $\mathbf{B}_0/B_0$ is neglected. However, the magnetic field line can be curved, for example, in a magnetic fusion plasma [43–46] or space plasma. [47–49] In order to take into account the geometric effects, the dielectric tensor can be obtained in a curvilinear geometry with a finite $\nabla(\mathbf{B}_0/B_0)$ term. The geometric effects on the dispersion relation and instability for a non-uniform plasma will be shown in future work.

Acknowledgments

This work was supported by the U.S. DOE under Grant Nos. DE-SC0022048 and DE-FG02-04ER54746, and the National Research Foundation of Korea under BK21+.

Appendix

This appendix provides the detailed derivations of equations (7), (10)-(14). Note that the species subscript a will be omitted for simplicity.

Using the equilibrium momentum equation (6), the linearized momentum equation,

$$\begin{aligned} & n_0 m \frac{\partial \mathbf{u}_1}{\partial t} + n_1 m \mathbf{u}_0 \cdot \nabla \mathbf{u}_0 \\ & + n_0 m \mathbf{u}_1 \cdot \nabla \mathbf{u}_0 + n_0 m \mathbf{u}_0 \cdot \nabla \mathbf{u}_1 \\ & = n_0 q (\mathbf{E}_1 + \mathbf{u}_0 \times \mathbf{B}_1 + \mathbf{u}_1 \times \mathbf{B}_0) \\ & + n_1 q (\mathbf{E}_0 + \mathbf{u}_0 \times \mathbf{B}_0) - \nabla \cdot \mathsf{p}_1, \end{aligned} \tag{A.1}$$

can be recast as

$$M_1 = M_2 + M_3, \tag{A.2}$$

where

$$\begin{aligned} M_1 = & \frac{\partial \mathbf{u}_1}{\partial t} + \mathbf{u}_1 \cdot \nabla \mathbf{u}_0 + \mathbf{u}_0 \cdot \nabla \mathbf{u}_1 \\ & - \frac{q}{m} \mathbf{u}_1 \times \mathbf{B}_0 - \frac{n_1}{n_0} \frac{\nabla \cdot \mathsf{p}_0}{m n_0}, \\ M_2 = & \frac{q}{m} (\mathbf{E}_1 + \mathbf{u}_0 \times \mathbf{B}_1), \\ M_3 = & - \frac{\nabla \cdot \mathsf{p}_1}{m n_0}. \end{aligned} \tag{A.3}$$

The first term M_1 can be rearranged as

$$\begin{aligned} M_1 = & - \mathrm{i}\, \omega_D \left[\mathsf{I} + \mathrm{i} \frac{\omega_c}{\omega_D} \hat{z} \times \mathsf{I} + \frac{\mathrm{i}}{\omega_D} \left((\nabla \mathbf{u}_0)^{\mathrm{T}} \right.\right. \\ & \left.\left. - \frac{\nabla \cdot \mathsf{P}_0}{m n_0} \frac{\mathbf{k} + \mathrm{i} \kappa_n}{\omega_D + \mathrm{i} \kappa_n \cdot \mathbf{u}_0} \right) \right] \cdot \mathbf{u}_1, \end{aligned} \tag{A.4}$$

where we have used the relations $\mathbf{u}_1 \cdot \nabla \mathbf{u}_0 = (\nabla \mathbf{u}_0)^{\mathrm{T}} \cdot \mathbf{u}_1$, $\mathbf{u}_0 \cdot \nabla \mathbf{u}_1 = \mathrm{i} \mathbf{k} \cdot \mathbf{u}_0 \mathbf{u}_1$, $-q \mathbf{u}_1 \times \mathbf{B}_0 / m = \omega_c \hat{z} \times \mathsf{I} \cdot \mathbf{u}_1$, and the linearized continuity equation (3). The perturbed magnetic field $\mathbf{B}_1$ can be replaced by $\mathbf{k}\times\mathbf{E}_1/\omega$ using the Faraday's law to give

$$M_2 = \omega_D \frac{q}{m\omega}\left(\mathsf{I}+\frac{\mathbf{k}\,\mathbf{u}_0}{\omega_D}\right)\cdot\mathbf{E}_1. \tag{A.5}$$

Since we consider a diagonal pressure tensor ($\mathsf{p} = p^{\perp}(\mathsf{I}-\hat{z}\hat{z}) + p^{\|}\,\hat{z}\hat{z}$) and neglect the geometric effect ($\nabla\cdot(\mathbf{B}_0\,\mathbf{B}_0/B_0^2) = 0$), the last term M_3 is written as

$$M_3 = -\mathrm{i}\,\frac{\mathbf{k}_{\perp}p_1^{\perp}+\mathbf{k}_{\|}p_1^{\|}}{m\,n_0}. \tag{A.6}$$

Combining equations (A.2) and (A.4)-(A.6) gives the linearized momentum equation (7).

The linearized pressure equations are obtained from the pressure equations (8) and (9) as

$$\begin{aligned}\frac{\partial p_1^{\perp}}{\partial t} &+ \mathbf{u}_0\cdot\nabla p_1^{\perp} + \mathbf{u}_1\cdot\nabla p_0^{\perp} + 2p_0^{\perp}\nabla\cdot\mathbf{u}_1\\ &+2p_1^{\perp}\nabla\cdot\mathbf{u}_0 - p_0^{\perp}\partial_{\|}\,u_{1\|} - p_1^{\perp}\partial_{\|}\,u_{0\|} = 0,\end{aligned} \tag{A.7}$$

$$\begin{aligned}\frac{\partial p_1^{\|}}{\partial t} &+ \mathbf{u}_0\cdot\nabla p_1^{\|} + \mathbf{u}_1\cdot\nabla p_0^{\|} + p_0^{\|}\nabla\cdot\mathbf{u}_1\\ &+p_1^{\|}\nabla\cdot\mathbf{u}_0 + 2p_0^{\|}\,\partial_{\|}\,u_{1\|} + 2p_1^{\|}\,\partial_{\|}\,u_{0\|} = 0,\end{aligned} \tag{A.8}$$

where the divergence of heat fluxes are neglected by the 6-moment approximation as discussed in section 2. Using the relations $\mathbf{u}_0\cdot\nabla p_1^{\perp,\|} = \mathrm{i}\mathbf{k}\cdot\mathbf{u}_0\,p_1^{\perp,\|}$, $\nabla\cdot\mathbf{u}_1 = \mathrm{i}\mathbf{k}\cdot\mathbf{u}_1$, and $\partial_{\|}\,u_{1\|} = \mathrm{i}\mathbf{k}_{\|}\cdot\mathbf{u}_1$, equations (A.7) and (A.8) can be rearranged to give the linearized pressure equations (10) and (11).

Since the perturbed pressures are expressed in terms of the perturbed flow velocity $\mathbf{u}_1$ in equations (10) and (11), equation (A.6) can be written as

$$\begin{aligned}M_3 = -\Bigg(&\frac{\mathrm{i}\,\mathbf{k}_{\perp}\left(2\mathbf{k}-\mathbf{k}_{\|}+\mathrm{i}\kappa_{p^{\perp}}\right)v_{T^{\perp}}^2/2}{\omega_D+\mathrm{i}\,2\nabla\cdot\mathbf{u}_0-\mathrm{i}\,\partial_{\|}u_{0\|}}\\ &+\frac{\mathrm{i}\,\mathbf{k}_{\|}\left(\mathbf{k}+2\mathbf{k}_{\|}+\mathrm{i}\kappa_{p^{\|}}\right)v_{T^{\|}}^2/2}{\omega_D+\mathrm{i}\nabla\cdot\mathbf{u}_0+\mathrm{i}\,2\partial_{\|}u_{0\|}}\Bigg)\cdot\mathbf{u}_1.\end{aligned} \tag{A.9}$$

Inserting equations (A.4),(A.5), and (A.9) into equation (A.2) yields

$$\begin{aligned}&\Bigg[\mathsf{I}+\mathrm{i}\frac{\omega_c}{\omega_D}\hat{z}\times\mathsf{I}\\ &+\mathrm{i}\frac{1}{\omega_D}\Bigg((\nabla\mathbf{u}_0)^{\mathrm{T}}-\frac{\nabla\cdot\mathsf{P}_0}{m\,n_0}\,\frac{\mathbf{k}+\mathrm{i}\kappa_n}{\omega_D+\mathrm{i}\kappa_n\cdot\mathbf{u}_0}\\ &+\frac{\mathrm{i}\,\mathbf{k}_{\perp}\left(2\mathbf{k}-\mathbf{k}_{\|}+\mathrm{i}\kappa_{p^{\perp}}\right)v_{T^{\perp}}^2/2}{\omega_D+\mathrm{i}\,2\nabla\cdot\mathbf{u}_0-\mathrm{i}\,\partial_{\|}u_{0\|}}\\ &+\frac{\mathrm{i}\,\mathbf{k}_{\|}\left(\mathbf{k}+2\mathbf{k}_{\|}+\mathrm{i}\kappa_{p^{\|}}\right)v_{T^{\|}}^2/2}{\omega_D+\mathrm{i}\nabla\cdot\mathbf{u}_0+\mathrm{i}\,2\partial_{\|}u_{0\|}}\Bigg)\Bigg]\cdot\mathbf{u}_1\\ &=\mathrm{i}\frac{q}{m\omega}\left(\mathsf{I}+\frac{\mathbf{k}\,\mathbf{u}_0}{\omega_D}\right)\cdot\mathbf{E}_1.\end{aligned} \tag{A.10}$$

It is seen that the mobility μ in equation (12) and the coefficient Γ in equation (13) are obtained by equation (A.10).

When the pressure is isotropic, the linearized pressure equation,

$$\begin{aligned}\frac{\partial p_1}{\partial t} &+ \mathbf{u}_0 \cdot \nabla p_1 + \mathbf{u}_1 \cdot \nabla p_0 \\ &+\frac{5}{3} p_0 \nabla \cdot \mathbf{u}_1 + \frac{5}{3} p_1 \nabla \cdot \mathbf{u}_0 = 0,\end{aligned} \tag{A.11}$$

gives the perturbed pressure

$$\frac{p_1}{p_0} = \frac{5\mathbf{k}/3 + \mathrm{i}\kappa_p}{\omega_D + \mathrm{i}5\nabla \cdot \mathbf{u}_0/3} \cdot \mathbf{u}_1. \tag{A.12}$$

Since equation (A.6) is written as

$$M_3 = -\mathrm{i}\frac{\mathbf{k}p_1}{mn_0}, \tag{A.13}$$

the coefficient Γ for an isotropic pressure becomes equation (14).

References

[1] T. H. Stix. *Waves in Plasmas*. American Inst. of Physics, 1992.

[2] A. K. Sen, J. Chen, and M. Mauel. Production and identification of the ion-temperature-gradient instability. *Phys. Rev. Lett.*, 66:429–432, Jan 1991.

[3] Cintia Quireza, Robert T. Rood, T. M. Bania, Dana S. Balser, and Walter J. Maciel. The electron temperature gradient in the galactic disk. *The Astrophysical Journal*, 653(2):1226–1240, dec 2006.

[4] Christiane Schröder, Thomas Klinger, Dietmar Block, Alexander Piel, Gérard Bonhomme, and Volker Naulin. Mode selective control of drift wave turbulence. *Phys. Rev. Lett.*, 86:5711–5714, Jun 2001.

[5] J. Vranjes and S. Poedts. Drift waves in the corona: heating and acceleration of ions at frequencies far below the gyrofrequency. *Monthly Notices of the Royal Astronomical Society*, 408(3):1835–1839, 10 2010.

[6] S Ayaz, Imran A Khan, Z Iqbal, and G Murtaza. Alfvén waves in temperature anisotropic cairns distributed plasma. *Communications in Theoretical Physics*, 72(3):035502, feb 2020.

[7] M.J. Hole, Z. Qu, S. Pinches, M. Schneider, I.L. Arbina, M.J. Mantsinen, and O. Sauter. The impact of anisotropy on ITER scenarios. *Nuclear Fusion*, 60(11):112010, aug 2020.

[8] Min Uk Lee, Jeong-Young Ji, and Gunsu S. Yun. Cold-hot coupled waves in a flowing magnetized plasma. *Nuclear Fusion*, 60(12):126036, oct 2020.

[9] W Zwingmann, L-G Eriksson, and P Stubberfield. Equilibrium analysis of tokamak discharges with anisotropic pressure. *Plasma Physics and Controlled Fusion*, 43(11):1441–1456, oct 2001.

[10] A. Bader, G. Stenberg Wieser, M. AndrÃ©, M. Wieser, Y. Futaana, M. Persson, H. Nilsson, and T. L. Zhang. Proton temperature anisotropies in the plasma environment of venus. *Journal of Geophysical Research: Space Physics*, 124(5):3312–3330, 2019.

[11] C. B. Beatty, T. E. Steinberger, E. M. Aguirre, R. A. Beatty, K. G. Klein, J. W. McLaughlin, L. Neal, and E. E. Scime. Creation of large temperature anisotropies in a laboratory plasma. *Physics of Plasmas*, 27(12):122101, 2020.

[12] David S. Montgomery. Two decades of progress in understanding and control of laser plasma instabilities in indirect drive inertial fusion. *Physics of Plasmas*, 23(5):055601, 2016.

[13] Thomas Hayward-Schneider, Philipp Lauber, Alberto Bottino, and Alexey Mishchenko. Multi-scale analysis of global electromagnetic instabilities in iter pre-fusion-power operation plasmas. *Nuclear Fusion*, 2022.

[14] Daniel Verscharen, Kristopher G. Klein, and Bennett A. Maruca. The multi-scale nature of the solar wind. *Living Reviews in Solar Physics*, 16(1):5, 2019.

[15] W. Biel, R. Albanese, R. Ambrosino, M. Ariola, M.V. Berkel, I. Bolshakova, K.J. Brunner, R. Cavazzana, M. Cecconello, S. Conroy, A. Dinklage, I. Duran, R. Dux, T. Eade, S. Entler, G. Ericsson, E. Fable, D. Farina, L. Figini, C. Finotti, Th. Franke, L. Giacomelli, L. Giannone, W. Gonzalez, A. Hjalmarsson, M. Hron, F. Janky, A. Kallenbach, J. Kogoj, R. KÃ¶nig, O. Kudlacek, R. Luis, A. Malaquias, O. Marchuk, G. Marchiori, M. Mattei, F. Maviglia, G. De Masi, D. Mazon, H. Meister, K. Meyer, D. Micheletti, S. Nowak, Ch. Piron, A. Pironti, N. Rispoli, V. Rohde, G. Sergienko, S. El Shawish, M. Siccinio, A. Silva, F. da Silva, C. Sozzi, M. Tardocchi, M. Tokar, W. Treutterer, and H. Zohm. Diagnostics for plasma control - from iter to demo. *Fusion Engineering and Design*, 146:465–472, 2019. SI:SOFT-30.

[16] L. Shi, E. J. Valeo, B. J. Tobias, G. J. Kramer, L. Hausammann, W. M. Tang, and M. Chen. Synthetic diagnostics platform for fusion plasmas (invited). *Review of Scientific Instruments*, 87(11):11D303, 2016.

[17] Min Uk Lee, Shekar G. Thatipamula, Sehyun Bae, Jayhyun Kim, Jaewook Kim, Michael Lehnen, and Gunsu S. Yun. Radiation measurement in plasma disruption by thin-foil infrared bolometer. *Review of Scientific Instruments*, 92(5):053536, 2021.

[18] M. Lazar, P. H. Yoon, R. A. López, and P. S. Moya. Electromagnetic electron cyclotron instability in the solar wind. *Journal of Geophysical Research: Space Physics*, 123(1):6–19, 2018.

[19] Maksimovic, M., Bale, S. D., Chust, T., Khotyaintsev, Y., Krasnoselskikh, V., Kretzschmar, M., Plettemeier, D., Rucker, H. O., Soucek, J., Steller, M., Stverák, S., Trávnícek, P., Vaivads, A., Chaintreuil, S., Dekkali, M., Alexandrova, O., Astier, P.-A., Barbary, G., Bérard, D., Bonnin, X., Boughedada, K., Cecconi, B., Chapron, F., Chariet, M., Collin, C., de Conchy, Y., Dias, D., Guéguen, L., Lamy, L., Leray, V., Lion, S., Malac-Allain, L. R., Matteini, L., Nguyen, Q. N., Pantellini, F., Parisot, J., Plasson, P., Thijs, S., Vecchio, A., Fratter, I., Bellouard, E., Lorfèvre, E., Danto, P., Julien, S., Guilhem, E., Fiachetti, C., Sanisidro, J., Laffaye, C., Gonzalez, F., Pontet, B., Quéruel, N., Jannet, G., Fergeau, P., Brochot, J.-Y., Cassam-Chenai, G., Dudok de Wit, T., Timofeeva, M., Vincent, T., Agrapart, C., Delory, G. T., Turin, P., Jeandet, A., Leroy, P., Pellion, J.-C., Bouzid, V., Katra, B., Piberne, R., Recart, W., Santolík, O., Kolmasová, I., Krupar, V., Kruparová, O., Písa, D., Uhlír, L., Lán, R., Base, J., Ahlèn, L., André, M., Bylander, L., Cripps, V., Cully, C., Eriksson, A., Jansson, S.-E., Johansson, E. P. G., Karlsson, T., Puccio, W., Brínek, J., Öttacher, H., Panchenko, M., Berthomier, M., Goetz, K., Hellinger, P., Horbury, T. S., Issautier, K., Kontar, E., Krucker, S., Le Contel, O., Louarn, P., Martinovi´c, M., Owen, C. J., Retino, A., Rodríguez-Pacheco, J., Sahraoui, F., Wimmer-Schweingruber, R. F., Zaslavsky, A., and Zouganelis, I. The solar orbiter radio and plasma waves (rpw) instrument. *A&A*, 642:A12, 2020.

[20] G. T. Roberg-Clark, J. F. Drake, M. Swisdak, and C. S. Reynolds. Wave generation and heat flux suppression in astrophysical plasma systems. *The Astrophysical Journal*, 867(2):154, 2018.

[21] Stella Koch Ocker, James M. Cordes, Shami Chatterjee, Donald A. Gurnett, William S. Kurth, and Steven R. Spangler. Persistent plasma waves in interstellar space detected by voyager 1. *Nature Astronomy*, 5(8):761, 2021.

[22] G. Ganguli, Y. C. Lee, and P. J. Palmadesso. Kinetic theory for electrostatic waves due to transverse velocity shears. *The Physics of Fluids*, 31(4):823–838, 1988.

[23] D. G. Swanson. *Plasma Waves, 2nd Edition*. Series in Plasma Physics. Taylor & Francis, 2003.

[24] V. S. Mikhailenko, D. V. Chibisov, and V. V. Mikhailenko. Shear-flow-driven ion cyclotron instabilities of magnetic field-aligned flow of inhomogeneous plasma. *Physics of Plasmas*, 13(10):102105, 2006.

[25] V. V. Mikhailenko, V. S. Mikhailenko, and H. J. Lee. The combined kinetic effects of the ion temperature gradient and the velocity shear of a plasma flow parallel to the magnetic field on the drift-alfven instabilities. *Physics of Plasmas*, 27(11):112103, 2020.

[26] Min Uk Lee, Gunsu S Yun, and Jeong-Young Ji. Nonlinear harmonics coupled by parallel wave propagations in a time-dependent plasma flow. *Plasma Physics and Controlled Fusion*, 64(5):055005, mar 2022.

[27] R O Dendy. Interpretation of ion cyclotron emission from fusion and space plasmas. *Plasma Physics and*

Controlled Fusion, 36(12B):B163–B172, dec 1994.

[28] B Chapman, R O Dendy, S C Chapman, L A Holland, S W A Irvine, and B C G Reman. Comparing theory and simulation of ion cyclotron emission from energetic ion populations with spherical shell and ring-beam distributions in velocity-space. *Plasma Physics and Controlled Fusion*, 62(5):055003, mar 2020.

[29] R O Dendy and K G McClements. Ion cyclotron emission from fusion-born ions in large tokamak plasmas: a brief review from JET and TFTR to ITER. *Plasma Physics and Controlled Fusion*, 57(4):044002, mar 2015.

[30] G. F. Chew, M. L. Goldberger, F. E. Low, and Subrahmanyan Chandrasekhar. The boltzmann equation an d the one-fluid hydromagnetic equations in the absence of particle collisions. *Proceedings of the Royal Society of London. Series A. Mathematical and Physical Sciences*, 236(1204):112–118, 1956.

[31] P. M. Bellan. A microscopic, mechanical derivation of the adiabatic gas relation. *American Journal of Physics*, 72(5):679–682, 2004.

[32] P. Hunana, A. Tenerani, G. P. Zank, E. Khomenko, M. L. Goldstein, G. M. Webb, P. S. Cally, M. Collados, M. Velli, L. Adhikari, and et al. An introductory guide to fluid models with anisotropic temperatures. part 1. cgl description and collisionless fluid hierarchy. *Journal of Plasma Physics*, 85(6):205850602, 2019.

[33] W. Horton. Drift waves and transport. *Rev. Mod. Phys.*, 71:735–778, Apr 1999.

[34] J.-Y. Ji and E. D. Held. A framework for moment equations for magnetized plasmas. *Physics of Plasmas*, 21(4):042102, Apr 2014.

[35] A. Cardinali, S. Briguglio, G. Calabrò, F. Crisanti, C. Di Troia, G. Fogaccia, M. Marinucci, G. Vlad, and F. Zonca. Minority heating by ICRH: a tool for investigating burning plasma physics in FAST. *Nuclear Fusion*, 49(9):095020, sep 2009.

[36] Z. S. Qu, M. Fitzgerald, and M. J. Hole. Analysing the impact of anisotropy pressure on tokamak equilibria. *Plasma Physics and Controlled Fusion*, 56(7):075007, may 2014.

[37] L. Matteini, P. Hellinger, S. Landi, P. M. Tràvnìček, and M. Velli. Ion kinetics in the solar wind: Coupling global expansion to local microphysics. *Space Sci. Rev.*, 172(373), 2012.

[38] L. Sironi and R. Narayan. Electron heating by the ion cyclotron instability in collisionless accretion flows. I. compression-driven instabilities and the electron heating mechanism. *The Astrophysical Journal*, 800(2):88, feb 2015.

[39] P. M. Bellan. *Fundamentals of Plasma Physics*. Cambridge University Press, 2008.

[40] S. Shinohara. Propagating wave characteristics for plasma production in plasma processing field. *Japanese Journal of Applied Physics*, 36(Part 1, No. 7B):4695–4703, jul 1997.

[41] M. Kretzschmar, T. Chust, V. Krasnoselskikh, D. Graham, L. Colomban, M. Maksimovic, Yu. V. Khotyaintsev, J. Soucek, K. Steinvall, O. Santolík, G. Jannet, J.-Y. Brochot, O. Le Contel, A. Vecchio, X. Bonnin, S. D. Bale, C. Froment, A. Larosa, M. Bergerard-Timofeeva, P. Fergeau, E. Lorfevre, D. Plettemeier, M. Steller, S. Stverák, P. Trávnícek, A. Vaivads, T. S. Horbury, H. ÓBrien, V. Evans, V. Angelini, C. J. Owen, and P. Louarn. Whistler waves observed by solar orbiter/rpw between 0.5 au and 1 au. *A&A*, 656:A24, 2021.

[42] P H Diamond, S-I Itoh, K Itoh, and T S Hahm. Zonal flows in plasma—a review. *Plasma Physics and Controlled Fusion*, 47(5):R35–R161, apr 2005.

[43] D. A. Garren and A. H. Boozer. Magnetic field strength of toroidal plasma equilibria. *Physics of Fluids B: Plasma Physics*, 3(10):2805–2821, 1991.

[44] Allen H. Boozer. Non-axisymmetric magnetic fields and toroidal plasma confinement. *Nuclear Fusion*, 55(2):025001, jan 2015.

[45] A. Fasoli, S. Brunner, W. A. Cooper, J. P. Graves, P. Ricci, O. Sauter, and L. Villard. Computational challenges in magnetic-confinement fusion physics. *Nature Physics*, 12(5):411–423, May 2016.

[46] T. Andreeva, J. Geiger, A. Dinklage, G. Wurden, H. Thomsen, K. Rahbarnia, J.C. Schmitt, M. Hirsch, G. Fuchert, C. NÃŒhrenberg, A. Alonso, C.D. Beidler, M.N.A. Beurskens, S. Bozhenkov, R. Brakel, C. Brandt, V. Bykov, M. Grahl, O. Grulke, C. Killer, G. Kocsis, T. Klinger, A. Krämer-Flecken, S. Lazerson, M. Otte, N. Pablant, J. Schilling, T. Windisch, and the W7-X Team. Magnetic configuration

scans during divertor operation of wendelstein 7-X. *Nuclear Fusion*, 62(2):026032, jan 2022.

[47] Shijun Yoshida, Shin'ichirou Yoshida, and Yoshiharu Eriguchi. Twisted-torus equilibrium structures of magnetic fields in magnetized stars. *The Astrophysical Journal*, 651(1):462–474, nov 2006.

[48] P. M. Bellan, M. Livio, Y. Kato, S. V. Lebedev, T. P. Ray, A. Ferrari, P. Hartigan, A. Frank, J. M. Foster, and P. NicolaÃ¯. Astrophysical jets: Observations, numerical simulations, and laboratory experiments. *Physics of Plasmas*, 16(4):041005, 2009.

[49] Riddhi Bandyopadhyay, Yan Yang, William H. Matthaeus, Alexandros Chasapis, Tulasi N. Parashar, Christopher T. Russell, Robert J. Strangeway, Roy B. Torbert, Barbara L. Giles, Daniel J. Gershman, Craig J. Pollock, Thomas E. Moore, and James L. Burch. In situ measurement of curvature of magnetic field in turbulent space plasmas: A statistical study. *The Astrophysical Journal*, 893(1):L25, apr 2020.